POWER FLOW FUNDAMENTALS

INTRODUCTORY COMMENTS AND BACKGROUND

Introduction

The loading of the transmission components of an electric power system comprises the "power flow" of the network. The term "load flow" was coined before the use of computers when the load was actually moved from the demand site to the generation sites. Originally, a small physical model of the power system was built with equivalent resistors, inductors, and capacitors. Then the "solution" of the flows was achieved by measuring the current in each wire as a model was built for a segment of the system. The segments were then added using the superposition theorem of circuit theory to provide a complete solution. This procedure was tedious. It was also quite tricky as 120 V was normally the source because it was available "at the wall." As demand was added, the equivalent method was to find the impact of each new load (demand) on the generation. As load is added to the system, only the impact of the new load had to be emulated. Thus, the load was "flowed" from the load location back to each generator.

Generally, a power flow study assumes knowledge of bus loading and generation schedule at all buses except one. An example one-line diagram is shown in Fig. 1. The major substations, the power plants, and the transmission lines connecting the substations are often shown on a geographic map. All system interconnections are modeled with equivalents, if not calculated directly. Knowledge of all equipment model parameters, such as impedances or admittances, is required. A power flow uses the knowledge of load at each bus, the parameters for each piece of equipment (dependent current sources, dependent voltage sources, ideal transformers, resistances, reactances, and capacitances), and the power capability of each piece of equipment or device to determine a solution to the power flow equations. The power flow equations are an alternative statement of conservation of energy.

The transmission network includes all equipment that is interconnected to allow flow in both directions. The transmission network usually includes an equivalent model of the power system interconnections too remote to be of direct concern. Given the cost of computer capabilities, it is very common to study networks in excess of 30,000 buses. The nodes of the equivalent circuit are termed buses and are shown as dark bold lines in the above diagram. The branches between the buses are the transmission lines, the most common element, and are shown as light lines in the above diagram. Other devices, such as transformers, use alternative symbols as shown below.

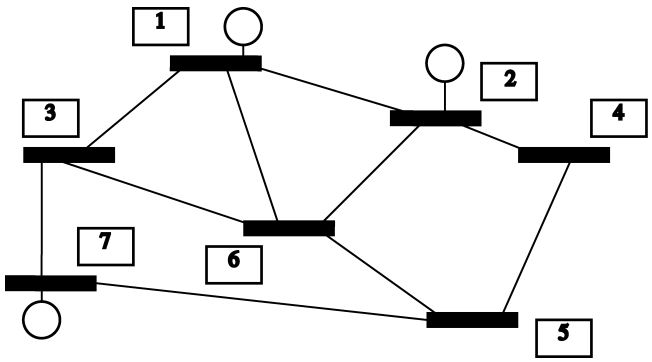

Figure 1. One-line diagram.

Generally, three-phase (3Φ) alternating current (AC) grids are used for electric power transmission, and power flow studies rely on a single-phase equivalent circuit representation. Such a model is only valid when the system is operating in a balanced mode where the other phases have the same voltages and currents are shifted by +/−120 degrees. The other phases may be obtained by simple addition or subtraction depending on the transformation used to obtain the per-phase equivalent. As the system is in a balanced mode, only the positive sequence network is included. Per unit equations are used throughout this section. The sum of the power flowing into a bus (node) must be zero. Alternatively, the power flowing out of a bus has to be zero, which is commonly referred to as "Tellegen's theorem."

When power conversion devices are used, such as direct current (DC) links or flexible alternating current (AC) transmission equipment, the power flow study solution methods must be modified to accommodate the rectifiers, inverters, and any series device such as a DC line. Some auxiliary equipment such as reactors, line filters, and interphase transformers may also be included as needed to provide an accurate solution.

Power conversion devices are now used for many transmission and distribution control applications based on advances in electronics. Power electronic devices originally included A/DC conversion equipment as used for DC links. However, more interesting devices control the flow on the transmission or distribution network. Such devices are referred to as flexible alternating current transmission (FACT) devices. These devices are based on technology similar to the A/DC converters. FACT devices can be categorized as series or shunt devices. Series devices are connected such that the power flow through the device is controlled. One example is to use series devices to control the real and/or reactive power through the transmission system to maintain the stability of the system or to limit flows between areas. Shunt devices are connected to ground to vary the equivalent demand at critical points of the network. Shunt devices are used to compensate customer loads that place unusual power demands on the transmission system.

Power flow studies are twofold: First, the high-voltage equipment is modeled and a solution is found; and second, the studies are extended to determine control settings to achieve the desired operating state. Studies in an operational setting determine what the control settings should be for the given equipment. Studies in a planning environment determine which equipment should be added to provide more secure and reliable operation for various future conditions.

Operational planning is given a specified system condition. The basic questions sought from a power flow study

are as follows:

- What are the line and transformer loads throughout the system?
- What are the voltages throughout the system?
- What are the options to unload overloaded equipment?
- What are the options to provide continued service as equipment fails unexpectedly?

Planning engineers are particularly interested in answering these questions as they evaluate proposed changes to an existing system, which are required as the demand increases as cities and industry expand or renovate:

- Which new generation sites provide the best operating solution on average and under adverse conditions?
- Which new transmission line locations provide the best operating solution on average and under adverse conditions?
- Which new DC links provide the best energy flows between areas?
- Which new FACTS devices will provide the necessary control to maintain the system in a secure operating system?
- Where can new load locations be added given the current system design?

Electrical networks of R, L, and C elements model most power system equipment. It is thus very tempting to use either conventional loop or nodal analysis methods to solve for voltages and currents. Indeed, the basic circuit element analysis by phasor representation is applicable. However, this direct approach is not applicable because the demands are known as complex powers. This special case is of a dependent current source where the independent variable is the voltage being solved. The generators should not be modeled as "voltage sources." They behave like "power sources." The generator will provide the real power independent of the voltage or current required and will provide the reactive power needed to sustain the voltage desired within capability limits of the voltage control at the generator. The problem is to solve $2n$ nonlinear algebraic equations in $2n$ unknowns for an n bus system, which requires advanced numerical analysis techniques as optimal ordering of the equations for numerical stability and scarcity programming for efficient matrix manipulation.

The primary model of interest is the high-voltage alternating current transmission line and transformer. These systems can carry and convert large amounts of electric power. The high-voltage alternating current transmission line is modeled as four ideal circuit elements (capacitor, resistor, inductor, and capacitor). This model is shown in Fig. 7. The model for a transformer is composed of three ideal circuit elements (resistor, inductor, and ideal transformer). This model is shown in Fig. 8.

The secondary model of interest is the high-voltage electronic device that can convert and carry a large amount of electric power by synchronous switching of the three-phase

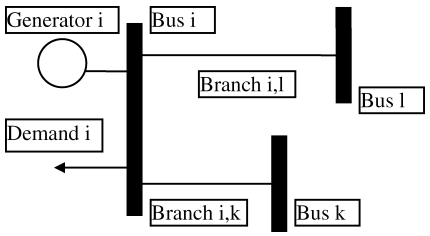

Figure 2. One-line diagram for a single bus.

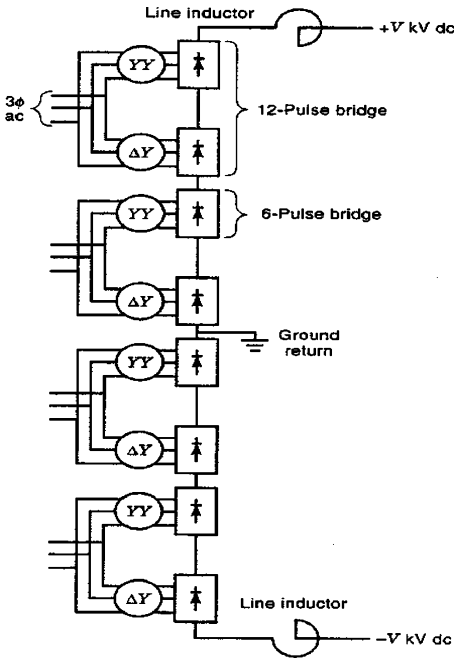

Figure 3. Converter system.

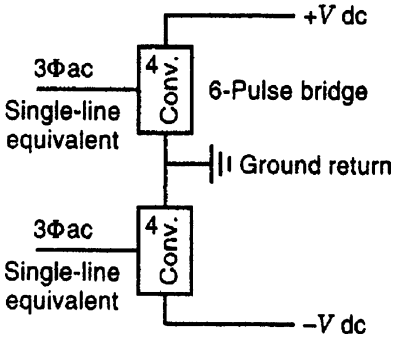

Figure 4. Single-line bipolar model.

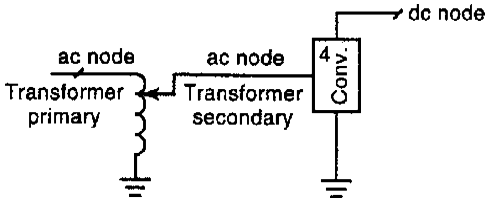

Figure 5. Monopole model.

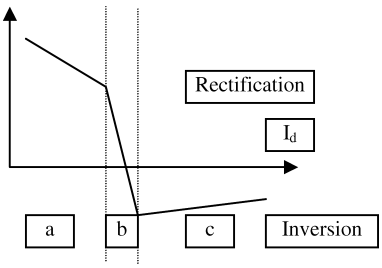

Figure 6. HVDC converter control characteristics; (a) constant ignition angle, (b) constant current, and (c) constant extinction.

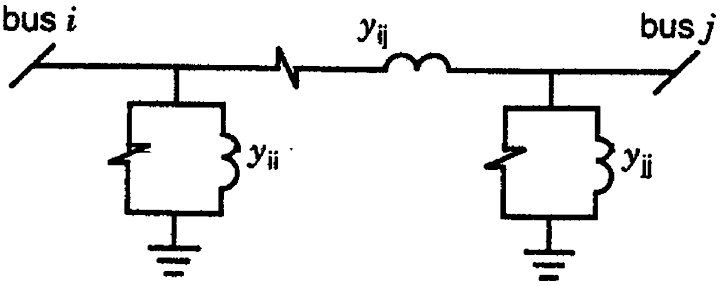

Figure 7. Transmission model.

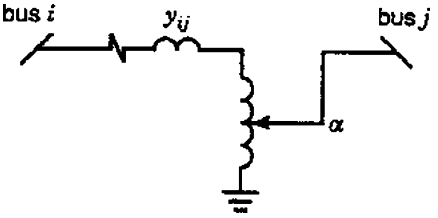

Figure 8. Transformer model.

voltage input. Most original converters were mercury arc tubes devices, but all new equipment is based on solid-state thyristors (1).

High-voltage direct current static converters have been commercially used for over 50 years. Various techniques for simulating high-voltage direct current (HVDC) systems on transient network analyzers, analog and hybrid computers, and digital computers have been documented in the literature. Transient network analyzers (TNAs) have traditionally been a popular means of studying interconnected AC–DC systems. Two common approaches exist: Either model the total converter system or model the converter system as an equivalent power source(s) plus load(s) of the system to be simulated. Many advances have been achieved to simulate all aspects of FACT devices. One of the first total solutions of composite AC/DC system simultaneously was in 1974 (1).

Earlier approaches solved the systems independently. Erich Uhlmann presented such an approach (2). The method essentially is to calculate the equivalent current sources and loads that the DC system could require of the AC system. The equivalent current sources and loads could be simulated on the TNA, because digital computer models were not available.

HVDC systems have been modeled in detail (3). The method is to design model components that are the miniature equivalents of actual equipment. Silicon controlled rectifiers in the normal bridge or Graetz circuit modeled the converters. Analog and hybrid computers had been used extensively to study HVDC systems because of the fast time response of the control equipment and the valves themselves. The wide-band hybrid computer enables the solution of the differential equations of the converter and control system approximately 300 times faster than digital computer software (4) available in the early 1970s. The hybrid computer and the transient network analyzer have a major drawback in the limitation on the size of the system that may be studied. Thus, extensive research, design, and implementation have been expended on modeling all equipment with digital computer models.

Digital computer programs now exist for the solution of the steady-state power flow of systems containing up to 100,000 buses. The installation of HVDC systems has increased significantly on the North American continent over the last four decades. The operating experience of the original Pacific DC Intertie, a bipolar $\pm$ 400 kV, 1440 MW system, has shown such systems to be very economic and reliable (5). Many similar HVDC links have been added around the world. HVDC links are often selected to provide service in underwater high-power cables (Sweden, New Zealand) and long-distance heavily loaded lines (Canada, United States, West Africa, Sweden, and Soviet Union).

The economy and reliability of HVDC systems has encouraged the consideration of FACT devices. Several

FACTs devices have been installed for experimental fact finding. The benefits of such systems are numerous. The costs of these systems are approaching the economic breakeven point to provide more reliable service based on the added flexibility (optionality) of this equipment. Thus, it is evident that computer power flow programs should be extended to handle all such equipment as FACT devices.

Conservation of Energy (Tellegen's Theorem)

The basic building block is the notion of conservation of energy (COE) at a bus and for the system as a whole. The starting equation is the conservation of energy at a bus as written by the summation of the complex power:

$$\sum_{j=k}^{l} \overline{S}_{ij} = 0$$

where the complex power is the summation of the real and the reactive power:

$$\overline{S} = P + Q\sqrt{-1}$$

Alternatively, the conservation of energy can be written as two summations, one for the real power and one for the reactive power:

$$\begin{aligned} \sum_{j=k}^{l} \overline{P}_{ij} &= 0 \\ \sum_{j=k}^{l} \overline{Q}_{ij} &= 0 \end{aligned}$$

Figure 2 shows the analysis at one bus to show conservation of energy at one bus.

The complex form for this bus follows:

$$\overline{S}_{gen,i} - \overline{S}_{demand,i} - \overline{S}_{ik} - \overline{S}_{il} = 0$$

The real forms are found from the application of the definition for complex (apparent), real, and reactive power. Thus, COE in the real forms follow:

$$\begin{aligned} \overline{P}_{gen,i} - \overline{P}_{demand,i} - \overline{P}_{ik} - \overline{P}_{il} &= 0 \\ \overline{Q}_{gen,i} - \overline{Q}_{demand,i} - \overline{Q}_{ik} - \overline{Q}_{il} &= 0 \end{aligned}$$

The power flow on any branch connecting any two buses is found as the series flow and the shunt flow as found from the π equivalent circuit of a transmission line as shown in the model development section. The conservation at each bus, except for the slack bus, is the key equation for the power flow formulation. The slack bus is also known as the swing bus.

Existing Techniques

Several techniques enable the study of electric systems and interconnections on digital computers. The various techniques have a common basis: the separation of the system solution into two sets of linear equations. The most widely used technique divides the real and reactive equations into two independent sets of equations. The first set is the real power equations. The second is the reactive power equations. Some techniques are in fact variants of the methods used to solve sets of simultaneous linear algebraic equations. A popular variant is the Gauss–Seidel technique that is related to relaxation techniques for simultaneous equation solution. The normal procedure is to solve the power system with the embedded control systems represented. Embedded controls traditionally included automatic control of voltage magnitude or of reactive flow by tap changing under load transformers. Other traditional embedded controls include real power flow control by quadrature phase-shifting transformers. Real and reactive power flow control by HVDC links is also solved as an embedded system within the last decade. Other FACT device controllers are currently included as embedded. Once the power system network is solved, then the extended control systems are solved and new values are calculated for the power flowing through each piece of equipment in a suboptimal manner. More recent power flow programs use optimizing algorithms to find the optimal control according to a desired performance index. Extended control systems include regional economic dispatch of generation to minimize production costs, regional shifting of generation to reduce power losses, and regional shifting of generation to reduce power flowing through overloaded equipment.

NEWTON–RAPHSON METHOD USING THE AUGMENTED JACOBIAN MATRIX

Power Flow Statement

Consider the ith bus of an n bus system. Tellegen's theorem requires that the energy at the bus must sum to zero:

$$\mathbf{S}_{Gi} = \mathbf{S}_{Li} + \mathbf{S}_{Ti} \tag{1}$$

where:

$\mathbf{S}_{Gi}$ complex generated power flowing into the bus.
$\mathbf{S}_{Li}$ complex demand power flowing out of the bus.
$\mathbf{S}_{Ti}$ complex transmitted power flowing out of the bus through network equipment over all connected links to adjacent buses.

(Bold letters represent complex variables.)

As the complex power can be separated into the real and the reactive components:

$$\mathbf{S}_{Gi} = \mathbf{P}_{Gi} + \mathrm{j}\,\mathbf{Q}_{Gi} \tag{2a}$$

$$\mathbf{S}_{Li} = \mathbf{P}_{Li} + \mathrm{j}\,\mathbf{Q}_{Li} \tag{2b}$$

$$\mathbf{S}_{Ti} = \mathbf{P}_{Ti} + \mathrm{j}\,\mathbf{Q}_{Ti} \tag{2c}$$

Then, it follows that the real and reactive equations may be solved independently:

$$\mathbf{P}_{Gi} = \mathbf{P}_{Li} + \mathbf{P}_{Ti} \tag{3a}$$

$$\mathbf{Q}_{Gi} = \mathbf{Q}_{Li} + \mathbf{Q}_{Ti} \tag{3b}$$

Note that both real and reactive powers are represented. Thus, six variables per bus exist whose relationship is dictated by two independent equations (10and 11). The system size grows dramatically! An n bus system will yield $2n$ equations involving $6n$ variables. The power flow solution is made at specified demand conditions. Therefore, P_{Li} and Q_{Li} are known. Four variables per bus exist: P_{Gi}, Q_{Gi}, P_{Ti}, and Q_{Ti}. The generation and demand terms are simple

constants for most buses. However, the transmission terms represent the real and reactive flow on equipment (transmission lines, transformers, inductors, capacitors, FACT devices, etc.) that are unique modeling problems. Note that generation and demand are external to the power flow relationships of the transmission network. The power system network is passive. It is treated as an n port network.

Many authors use either the impedance or the admittance matrix approach. Of these, the admittance method proves more suited. However, it is not necessary to use either the admittance or the impedance matrix explicitly. We will formulate our problem directly from the power flow relationship of each piece of equipment. The bus admittance matrix is not used in the following. Instead the branch admittance matrix is used. We will use the generic term link for any network element (transmission line, transformer, etc.). Tellegen's theorem (conservation of energy) for each bus can be rewritten to separate the known injections from the unknown flows:

$$\mathbf{P}_{\mathrm{Gi}} - \mathbf{P}_{\mathrm{Li}} = \mathbf{P}_{\mathrm{Ti}} \tag{4a}$$

$$\mathbf{Q}_{\mathrm{Gi}} - \mathbf{Q}_{\mathrm{Li}} = \mathbf{Q}_{\mathrm{Ti}} \tag{4b}$$

Consider a bus with m link connections in a power system:

$$\mathbf{S}_{Ti} = \sum_{j=1}^{m} \mathbf{S}_{ij} \tag{5}$$

The complex equipment flow in each piece of equipment is composed of a real and a reactive term:

$$\mathbf{S}_{\mathrm{ij}} = \mathbf{P}_{\mathrm{ij}} + \mathrm{j}\,\mathbf{Q}_{\mathrm{ij}} \tag{6}$$

The complex equipment flow is a function of the voltage at the bus and the complex conjugate of the current leaving the bus:

$$\mathbf{S}_{\mathrm{ij}} = \mathbf{V}_{\mathrm{i}}\mathbf{I}_{\mathrm{ij}}^{*} \tag{7}$$

The current is a function of the admittance between this bus and all other buses and the current to ground through the shunt impedance:

$$\mathbf{I}_{\mathrm{ij}} = \mathbf{Y}_{\mathrm{ii}}\mathbf{V}_{\mathrm{i}} + \mathbf{Y}_{\mathrm{ij}}(\mathbf{V}_{\mathrm{i}} - \mathbf{V}_{\mathrm{j}}) \tag{8}$$

We use the normal admittance notation relating the complex admittance to the real variables of conductance and susceptance: $\mathrm{Y} = \mathrm{g} + \mathrm{jb}$. Yii gives the admittance representing the equipment connected only to the node and Yij gives the admittance between the buses.

$$\mathbf{S}_{\mathrm{ij}} = \mathrm{V}_{\mathrm{i}}\mathrm{Y}_{\mathrm{ij}}^{*}\mathrm{V}_{\mathrm{i}}^{*} + \mathrm{V}_{\mathrm{i}}\mathrm{V}_{\mathrm{i}}\mathrm{Y}_{\mathrm{ii}}^{*} - \mathrm{V}_{\mathrm{i}}\mathrm{V}_{\mathrm{j}}^{*}\mathrm{Y}_{\mathrm{ij}}^{*} \tag{9}$$

Note that this includes the "self" term of the bus admittance matrix:

$$\mathrm{P}_{\mathrm{ij}} = \mathrm{V}_{\mathrm{i}}^{2}\mathrm{Y}_{\mathrm{ij}}\cos(-\gamma_{\mathrm{ij}}) - \mathrm{V}_{\mathrm{i}}\mathrm{V}_{\mathrm{j}}\mathrm{Y}_{\mathrm{ij}}\cos(\delta_{\mathrm{i}} - \delta_{\mathrm{j}} - \gamma_{\mathrm{ij}}) \tag{10a}$$

$$\mathrm{Q}_{\mathrm{ij}} = \mathrm{V}_{\mathrm{i}}^{2}\mathrm{Y}_{\mathrm{ij}}\sin(-\gamma_{\mathrm{ij}}) - \mathrm{V}_{\mathrm{i}}\mathrm{V}_{\mathrm{j}}\mathrm{Y}_{\mathrm{ij}}\sin(\delta_{\mathrm{i}} - \delta_{\mathrm{j}} - \gamma_{\mathrm{ij}}) - \mathrm{V}_{\mathrm{i}}^{2}\mathrm{Y}_{\mathrm{ii}} \tag{10b}$$

where $\mathrm{V_i}$ and $\mathrm{V_j}$ are the voltage magnitudes at bus i and bus j, $\mathrm{Y_{ij}}$ is the admittance magnitude of the link between bus i and bus j, δ_{i} and δ_{j} are the voltage angles at bus i and bus j, and γ_{ij} is the admittance angle of the link between bus i and bus j. Note that the summation of all admittances to a bus still constitutes the diagonal entry of the bus admittance matrix as is required of nodal analysis.

Note that we substitute the flow variables ($\mathrm{P_{Ti}}$, $\mathrm{Q_{Ti}}$) with the potential variables ($\mathrm{V_i}$, δ_{i}). The complexity of the power flow problem should now be apparent. The transmitted real and reactive power at a given bus will be a function of the voltage magnitude and angle at all other buses.

Six variables at each bus exist: $\mathrm{P_{Gi}}$, $\mathrm{Q_{Gi}}$, $\mathrm{P_{Li}}$, $\mathrm{Q_{Li}}$, $\mathrm{V_i}$, and δ_{i}. The demand is specified and is not normally altered. Such a model is based on the obligation to serve the principle of the traditionally regulated environment. However, note that it is the net real and reactive power injection at each bus that is balanced by the transmitted flows, which leaves four variables and two equations. Thus, two more variables need to be specified. Mathematically, any two variables may be selected. When each bus is examined, only variables that are known should be specified. The choice is dictated by the device(s) connected to a particular bus. Several options are summarized in Table 1. These options define bus types to signify the variables that are known.

The first type ($\mathrm{V}\delta$) is referred to as the swing or slack bus. It is normally a generator bus to satisfy the balance of demand and losses with generation. Thus, no constraints exist on the real or reactive power generated. One phasor quantity is selected as phase reference in any AC circuit. The generation required is determined by, setting the phase angle of the voltage to zero at the reference bus. It is also common to set the voltage magnitude to 1.0 per unit, because a generator normally has control of the voltage through the exciter. However, this is not necessary. The voltage magnitude may be solved if the reactive power is fixed. It is common practice to select a "tie" bus as the swing bus in some studies. A "tie" bus has no generation or demand attached. Thus, any real or reactive generation found after solution shows that the generation was not equal to the demand and losses. Then it would be necessary to redispatch the generation economically. Only one slack should be chosen per system island.

The type PQ bus would identify any bus for which $\mathrm{P_{Gi}}$ and $\mathrm{Q_{Gi}}$ are known. This type includes any bus with no generation. Type PQ busses are the most common. Solve for the unknown $\mathrm{V_i}$, δ_{i} variables at such buses.

The last bus type PV ("voltage controlled") is separated into two classifications because of control differences. The voltage can be controlled by an exciter at a generator bus, by a transformer, or by a FACT device. Different emulation calculations are used at these buses. The type PV bus is typically a bus with a generator connected to it. The two main control actions available at a generator plant enable control of $\mathrm{P_i}$, and $\mathrm{V_i}$. As these values are controlled, they should be specified as known. Generator operating characteristics require that the operation stay within the capability of the generator. Alternatively, other reactive power equipment may provide such control.

The limits on $\mathrm{Q_{Gi}}$ are unusual in that the reactive power to support a given voltage is not solved within the matrix calculations. Instead, it is calculated based on the latest update to the voltage magnitudes and angles. After this calculation, check to see whether the required reactive generation is within limits. If it is not within limits, set it at the appropriate limit and release the constraint that $\mathrm{V_i}$ is fixed. That is, $\mathrm{V_i}$ and $\mathrm{Q_{Gi}}$ exchange roles, which changes the type of the bus from PV to PQ. During subsequent it-

Table 1. Bus types for power flow formulation

Bus Type	Code	Knowns	Unknowns
Slack generator	Vδ	V_i, δ_i	P_{Gi}, Q_{Gi}
Slack demand or tie	Qδ	Q_{Gi}, δ_i	P_{Gi}, V_i
Demand	PQ	P_{Gi}, Q_{Gi}	V_i, δ_i
Generator	PV	P_{Gi}, V_i	Q_{Gi}, δ_i
Controlled voltage magnitude	CV	P_{Gi}, V_i	δ_i,α

Table 2. Power Flow Procedure

Step	Input	Process	Output
1	Equipment data	Merge into tables	Tabular data
2	Equipment data: Initial solution or latest solution	Build Jacobian matrix	Jacobian matrix
3	Equipment data: Initial solution or latest solution	Calculate residual mismatch at each bus	Net power injection at all buses, all power flows, and all control statuses
4	Maximum mismatch	Compare maximum mismatch with acceptable tolerance, check iteration count	Decision to continue with next iteration
5	Jacobian matrix as well as real and reactive power mismatches	Solve augmented Jacobian matrix	Updates to voltage magnitude and angle as well as control variable updates
6	Repeat Steps 2 through 6		

Table 3. Bus Data

Bus Number	|V| Magnitude	δ Angle	P Real Demand	Q Reactive Demand	B_{gr} Shunt Capacitance
1	1.05	0.00	0.952	0.436	0.033898
2	1.10	− 3.36	0.500	0.185	0.000000
3	1.00	−12.79	−0.550	−0.130	0.000000
4	0.93	− 9.84	0.000	0.000	0.029326
5	0.92	−12.34	−0.300	−0.180	0.000000
6	0.92	−12.24	−0.500	−0.050	0.035088

Table 4. Line Data

From Bus	To Bus	G Series admittance	B Series Susceptance	Tap Ratio
1	4	0.558269	−2.581996	0.0
1	6	0.433934	−1.827463	0.0
2	3	0.444860	−0.646063	0.0
2	5	0.576541	−1.308462	0.0
3	4	0.0	−7.518797	1.100
4	6	0.554102	−2.324944	0.0
5	6	0.0	−3.333333	1.025

erations, continue to check the reactive power needed to support the voltage desired. Whenever the required reactive power falls within acceptable limits, change the bus type to PV. Note that this process may occur more than once during a solution.

The second type of voltage control is a “CV” bus using a tap changing under load (TCUL) transformer. The real and reactive power at the bus is fixed, but the setting of the tap controls the voltage, which does change the bus type at the controlled bus to a CV. The bus is modeled as

Table 5. Line Power Flows

Bus	To Bus	P	Q
1	4	0.5091	0.2705
4	1	−0.4849	−0.1590
1	6	0.4431	0.2025
6	1	−0.4166	−0.0910
2	3	0.1718	−0.0001
3	2	−0.1541	0.0257
2	5	0.3283	0.1851
5	2	−0.2951	−0.1100
3	4	−0.3957	−0.1557
4	3	0.3957	0.1815
4	6	0.0891	0.0047
6	4	−0.0882	−0.0010
5	6	−0.0048	−0.0700
6	5	0.0048	0.0743

Table 6. HVDC Link Data

Bus	To Bus	X_K	Firing Angle (α)	Commutation ngle (γ)	G(series)
6	7	1.000	10°	20°	–
2	8	1.000	150°	20°	–
7	8	–	–	–	5.000

Table 7. Adjusted Bus Data

Bus Number	$\|E\|$	δ	P	Q	B_{gr}
1	1.05	0.0	0.849	0.577	0.033898
2	0.89	−7.80	0.600	0.650	0.000000
3	0.95	−13.99	0.550	0.130	0.000000
4	0.90	−9.80	0.000	0.000	0.029326
5	0.86	−12.98	0.300	0.180	0.000000
6	0.90	−8.82	0.500	0.650	0.035088
7	0.99	–	0.000	–	–
8	0.89	–	0.000	–	–

Table 8. HVDC Convert and HVDC Link Power Flows

Bus	To Bus	P	Q
28	82	0.4460−0.4460	0.7064−
67	76	−0.40500.4050	0.6415−
78	87	0.4460−0.4050	−−

normally done for the real power equation. However, the reactive equation is replaced by an equation relating the dependency between the voltage magnitude and the transformer tap ratio magnitude (α). Note that only one device should be controlling the voltage magnitude at a bus each iteration of the solution process. Such models are extended to FACT devices that provide similar control.

Mathematical Overview

The widely used method of solving AC power flow problems is the Newton–Raphson (Newton's point form) method (6, 7). The method relies on the solution of a vector-matrix nonlinear equation:

$$F(X) = 0 \tag{11}$$

where F is a vector-valued nonlinear function of a vector-valued argument X An initial guess $X^{(O)}$ gives the vector-matrix Taylor expansion of F(X) about X as:

$$F(X) = 0 = F(X^{(O)}) + J\Delta X + \text{higher order term}$$

$$(J)_{ij} = \frac{\partial F_i}{\partial X_j} \tag{12}$$

where J is the system Jacobian matrix, F_i is the ith component of F, and X_j is the jth component of X. In addition, ΔX is a first-order correction to $X^{(O)}$.

Table 9. AC Power Flows with HVDC Link

Bus	To Bus	P	Q
1	4	0.5115	0.3650
4	1	−0.4828	−0.2325
1	6	0.3385	0.2490
6	1	−0.3187	−0.1660
2	3	0.0398	0.0699
3	2	−0.0340	0.0783
2	5	0.1143	0.0135
5	2	−0.1096	−0.0030
3	4	−0.5160	−0.2083
4	3	0.5160	0.2066
4	6	−0.0332	0.0024
6	4	0.0333	−0.0019
5	6	−0.1904	−0.1771
6	5	0.1904	0.1481

Excluding the slack bus (node), there are usually two equations for each node of the form:

$$\begin{aligned} \Delta P_i &= \Sigma \frac{\partial P_{ij}}{\partial \delta_j} \Delta\delta_j + \Sigma V_j \frac{\partial P_{ij}}{\partial V_j} \frac{\Delta V_j}{V_j} \\ \Delta Q_i &= \Sigma \frac{\partial Q_{ij}}{\partial \delta_j} \Delta\delta_j + \Sigma V_j \frac{\partial Q_{ij}}{\partial V_j} \frac{\Delta V_j}{V_j} \end{aligned} \tag{13}$$

$$\begin{aligned} \Delta Pi &= Pi(\text{specified}) - Pi(\text{calculated}) \\ \Delta Qi &= Qi(\text{specified}) - Qi(\text{calculated}) \end{aligned}$$

where the summations are over all connections to adjacent buses j for the mismatch at bus i. The P_i (specified), Q_i (specified) is the net real and net reactive power at bus i. Thus, the procedure is to calculate the partials for each bus, calculate the ΔP_i and ΔQ_i for each bus by the above equations, and test for convergence (each residual less than a prespecified tolerance). This assembles a matrix of the general form (Eq. 29), where $(o)^T$ signifies transposition and A_t signifies a submatrix of matrix A. Note that (A) denotes an element of matrix A.

$$Ax = b$$

$$x = A^{-1}b \tag{14}$$

$$\begin{aligned} b &= [\Delta P_2,\ \Delta P_3, \ldots, \Delta P_n\, \Delta Q_2,\ \Delta Q_3, \ldots,\ \Delta Q_n]^T \\ x &= [\Delta\delta_2,\ \Delta\delta_3, \ldots, \Delta\delta_n,\ \frac{\Delta V_2}{V_2},\ \frac{\Delta V_3}{V_3}, \ldots,\ \frac{\Delta V_n}{V_n}]^T \end{aligned}$$

$$A = \begin{bmatrix} A_{ii} & A_{ij} \\ A_{ji} & A_{jj} \end{bmatrix} \tag{15}$$

$$A_{ii} = \begin{bmatrix} \frac{\partial P_{ii}}{\partial \delta_i} & V_i \frac{\partial P_{ii}}{\partial V_i} \\ \frac{\partial Q_{ii}}{\partial \delta_i} & V_i \frac{\partial Q_{ii}}{\partial V_i} \end{bmatrix} A_{ij} = \begin{bmatrix} \frac{\partial P_{ij}}{\partial \delta_j} & V_j \frac{\partial P_{ij}}{\partial V_j} \\ \frac{\partial Q_{ij}}{\partial \delta_j} & V_j \frac{\partial Q_{ij}}{\partial V_j} \end{bmatrix}$$

The next step is to solve the augmented matrix $[A \mid b]$ by Gaussian elimination. The equations are processed one bus (one ΔP_i and ΔQ_i equation) at a time. Using chain-linked data structures optimizes efficiency and speed. A well-known method for the rapid solution of these equations requires the back substitution of an augmented matrix (8–11), which completes the solution to find x (the voltage magnitude and angle for each bus).

AC System Control Modeling

The Newton–Raphson method has been expanded to directly simulate the steady-state effect of power system controls. The original work of Britton, Peterson, and Meyer provided an expanded view of the Newton–Raphson procedure as proposed by VanNess (12–14). The Britton paper presented a thorough development of over 12 control models for the power flow algorithm. Typical controls that are simulated include local and remote voltage control by reactive generation, line flow control by generation, local and remote voltage control by tap changing under load (TCUL) transformers, reactive line flow control by TCUL transformers, and real line flow control by phase-shifting transformers.

Local Voltage Control. The control model for local voltage control simulates a generating station's capability to maintain a specified voltage magnitude at the system bus to which it is connected. Thus there is only a real power equation ΔP with the partial derivative with respect to the voltage magnitude $\partial P/\partial V$ deleted because the voltage magnitude is constant:

$$\Delta P_i = \frac{\partial P_{ii}}{\partial \delta_i} \Delta\delta_i + \text{partials for adjacent buses} \tag{16}$$

Remote Voltage Control. There are cases in which a generator may control a system bus voltage magnitude even when that bus is not the terminal bus for that generator. A terminal bus is the system bus that has the generation represented as an injected power or current flow. The control and controlled system buses are sometimes referred to as a remote control pair. This option is one of the more complex ones to implement. The voltage magnitude at the controlled bus j is constant, and the real power equation has the partial derivatives with respect to the constant voltage magnitude deleted,

$$\Delta P_j = \frac{\partial P_{jj}}{\partial \delta_j} \Delta\delta_j + \text{partials for adjacent buses} \tag{17}$$

$$\Delta Q_j = \frac{\partial Q_{jj}}{\partial \delta_j} \Delta \delta_j + \text{partials for adjacent buses}$$

The control bus has only the real equation present because the reactive power constraint ΔQ is replaced by the load constraint for the controlled bus j above:

$$\Delta P_i = V_i \frac{\partial P_{ii}}{\partial V_i} \frac{\Delta V_i}{V_i} + \frac{\partial P_{ii}}{\partial \delta_i} \Delta \delta_i + \text{partials for adjacent buses} \tag{18}$$

Implementation was facilitated if the reactive power equation is processed as a "control equation" and not as an equation involving the parameters of the control node. This was the case because of the nature of the logic required in a digital implementation in order to accommodate active and reactive bus power constraints in an efficient manner.

Line and Area Interchange Power Flow. Line power flow control is obtained by letting a generator terminal bus vary its real and reactive generation. The nominal equation, for a generator terminal bus i, controlling a line from system bus j, to system bus k, is replaced by the equations:

$$\begin{aligned} \Delta P_{jk} &= V_j \frac{\partial P_{jk}}{\partial V_j} \frac{\Delta V_j}{V_j} + \frac{\partial P_{jk}}{\partial \delta_j} \Delta \delta_j + V_k \frac{\partial P_{jk}}{\partial V_k} \frac{\Delta V_k}{V_k} + \frac{\partial P_{jk}}{\partial \delta_k} \Delta \delta_k \\ \Delta Q_{jk} &= V_j \frac{\partial Q_{jk}}{\partial V_j} \frac{\Delta V_j}{V_j} + \frac{\partial Q_{jk}}{\partial \delta_j} \Delta \delta_j + V_k \frac{\partial Q_{jk}}{\partial V_k} \frac{\Delta V_k}{V_k} + \frac{\partial Q_{jk}}{\partial \delta_k} \Delta \delta_k \end{aligned} \tag{19}$$

These equations are the conventional expansions of the quantities ΔP_{ik} and ΔQ_{ik} in terms of all their arguments. Note that ΔP_{ij} and ΔQ_{ij} represent the difference between the scheduled and the calculated real and reactive power flow. The first use of this control model was the solution of the area interchange problem. The problem is to control the power flows in the transmission lines connecting power company A (area A) to power company B (area B). The solution is found by selecting a generator terminal bus either in area A or in area B to control the power flows between the two areas. Such a formulation is an area–area interchange model in which interchange at specific boundaries is constrained to a given schedule. An alternative formulation involves the control of the power flows from area A to all other areas. In this formulation, constraints on the total net interchange rather than the individual, inter-area interchange is scheduled. Note that net interchange implies the consideration of power flow into and out of an area. In this net interchange formulation, the solution is found by the selection of a generator terminal bus to control all tie lines of area A. The equations for the area interchange problems would be of the form:

$$\begin{aligned} \Delta P_{ab} &= \Sigma V_j \frac{\partial P_{jk}}{\partial V_j} \frac{\Delta V_j}{V_j} + \Sigma \frac{\partial P_{jk}}{\partial \delta_j} \Delta \delta_j + \Sigma V_k \frac{\partial P_{jk}}{\partial V_k} \frac{\Delta V_k}{V_k} + \Sigma \frac{\partial P_{jk}}{\partial \delta_k} \Delta \delta_k \\ \Delta Q_{ab} &= \Sigma V_j \frac{\partial Q_{jk}}{\partial V_j} \frac{\Delta V_j}{V_j} + \Sigma \frac{\partial Q_{jk}}{\partial \delta_j} \Delta \delta_j + \Sigma V_k \frac{\partial Q_{jk}}{\partial V_k} \frac{\Delta V_k}{V_k} + \Sigma \frac{\partial Q_{jk}}{\partial \delta_k} \Delta \delta_k \end{aligned} \tag{20}$$

where the summations are over all tie lines to be controlled. ΔP_{ab} and ΔQ_{ab} are the mismatch of the scheduled area interchanges. Traditionally, only the real power flow is controlled between areas.

Voltage Magnitude-Controlled Bus. TCUL transformers can control the voltage magnitude at a system node. Thus, the bus voltage magnitude is a constant, whereas the turns ratio α is variable. The equations of a system node k controlled by a TCUL between system nodes i and j are as follows:

$$\begin{aligned} \Delta P_k &= \alpha_{ij} \frac{\partial P_{ij}}{\partial \alpha_{ij}} \frac{\Delta \alpha_{ij}}{\alpha_{ij}} + \frac{\partial P_{kj}}{\partial \delta_i} \Delta \delta_i \\ &\quad + \text{partials for adjacent buses} \\ \Delta Q_k &= \alpha_{ij} \frac{\partial Q_{ij}}{\partial \alpha_{ij}} \frac{\Delta \alpha_{ij}}{\alpha_{ij}} + \frac{\partial Q_{kj}}{\partial \delta_i} \Delta \delta_i \\ &\quad + \text{partials for adjacent buses} \end{aligned} \tag{21}$$

This is only the replacement of the voltage-sensitive terms with the tap angle-sensitive terms. This result arises because ΔQ and ΔP are no longer functions of variable V, but instead they are functions of the variable α. Note that the controlled node does not have to be a terminal bus of the TCUL transformer. Then it would be necessary to know which terminal of the TCUL transformer is "closer electrically" to the controlled bus. Then the controlled bus equations would delete the partial derivative with respect to voltage magnitude and the equations for the terminal buses would have the above partial term in addition to their normal terms.

Line Power Flow by Transformer. Simulation of line power flow control, either by TCUL transformers or quadrature phase-shifting (QPS) transformers, requires that control equations be generated, which describe the line power flow in addition to the node parameters, AP, AQ. Note that a QPS transformer controls active power flow and that a TCUL transformer controls reactive power flow. The equation for a QPS at terminal nodes i and j, controlling a line between terminals i and j (therefore controlling itself), is of the form:

$$\begin{aligned} \Delta P_{ij} &= V_J \frac{\partial P_{ij}}{\partial V_j} \frac{\Delta V_j}{V_j} + \frac{\partial P_{ij}}{\partial \delta_j} \Delta \delta_j + V_i \frac{\partial P_{ij}}{\partial V_i} \frac{\Delta V_i}{V_i} + \frac{\partial P_{ij}}{\partial \delta_i} \Delta \delta_i \\ &\quad + \frac{\partial P_{ij}}{\partial \theta_{ij}} \Delta \theta_{ij} \end{aligned} \tag{22}$$

where the partial derivative of the flow with respect to the quadrature phase-shift angle is the last term. A TCUL transformer at terminal nodes i and j, controlling a line between terminals i and j (therefore controlling itself), is of the form:

$$\begin{aligned} \Delta Q_{ij} &= V_J \frac{\partial Q_{ij}}{\partial V_j} \frac{\Delta V_j}{V_j} + \frac{\partial P_{ij}}{\partial \delta_j} \Delta \delta_j + V_i \frac{\partial P_{ij}}{\partial V_i} \frac{\Delta V_i}{V_i} + \frac{\partial P_{ij}}{\partial \delta_i} \Delta \delta_i \\ &\quad + \alpha_{ij} \frac{\partial P_{ij}}{\partial \alpha_{ij}} \frac{\Delta \alpha_{ij}}{\alpha_{ij}} \end{aligned} \tag{23}$$

These control schemes can be expanded such that a QPS or a TCUL transformer can control a line other than itself and such that a set of lines can be controlled instead of a single line.

It is interesting to note that the QPS is almost entirely confined to use in the United States, almost entirely to the

Midwest and East. Its function is usually to control interchange power flow near heavy load centers.

Optimal Power Flow. An optimal power flow solves the COE equations while minimizing the economic cost of operation. The original approach was to use equations similar to the area interchange control (14). Other techniques use linear programming, quadratic programming, or interior point programming to optimize the objective function while maintaining the feasibility of the power flow equations.

HVDC Converter Model

The HVDC converter can be represented as a black box with a 3Φ AC line entering one side and one or two DC lines entering the other side (see Fig. 2) (15–17).

The black box represents either a 6π or a 12-pole converter that is capable of rectification or inversion. The actual converter system might be more accurately displayed as in Fig. 3. This example shows a bipolar, eight-bridge system. Steady-state operation can reduce the above diagram to a single line bipolar model shown in Fig. 4. Note that this representation is symmetric with respect to an axis drawn through the ground return, which suggests that a monopolar model, Fig. 5, could be adopted if the user accepted the task of reducing the system data to this model. One proposal is to use two monopolar models in Fig. 5 to represent the bipolar model in Fig. 4, which assumes that the ground return will not be a represented node in the power flow model. The equations for an AC bus i connected to a DC bus k are as follows:

$$\Delta P_i = \Sigma \frac{\partial P_{ij}}{\partial \delta_j} \Delta \delta_j + \Sigma V_j \frac{\partial P_{ij}}{\partial V_j} \frac{\Delta V_j}{V_j} + V_k \frac{\partial P_{ij}}{\partial V_k} \frac{\Delta V_k}{V_k} + \text{partials for adjacent buses}$$

$$\Delta Q_i = \Sigma \frac{\partial Q_{ij}}{\partial \delta_j} \Delta \delta_j + \Sigma V_j \frac{\partial Q_{ij}}{\partial V_j} \frac{\Delta V_j}{V_j} + V_k \frac{\partial Q_{ij}}{\partial V_k} \frac{\Delta V_k}{V_k} + \text{partials for adjacent buses} \quad (24)$$

The V_k is the average DC voltage measured with respect to ground. Compared with the general equations presented in the mathematical overview, the only change is the term corresponding to the phase-angle at bus k is missing. No reactive power is associated with any HVDC node in steady-state operation with ripple-free HVDC current. The equation for a DC node k, connected to an AC node i, and to another DC node j, by an HVDC transmission line is

$$\Delta P_k = V_i \frac{\partial P_{ki}}{\partial V_i} \frac{\Delta V_i}{V_i} + \frac{\partial P_{ki}}{\partial \delta_i} \Delta \delta_i + V_k \frac{\partial P_{kk}}{\partial V_k} \frac{\Delta V_k}{V_k} + V_k \frac{\partial P_{kj}}{\partial V_j} \frac{\Delta V_j}{V_j} \quad (25)$$

The DC node is solved only for the voltage magnitude as for any direct current circuit.

DC Control

Many alternatives may be used to control HVDC converters. The control schemes that may be employed are constant DC current (CC), constant DC power (CP), constant power factor at the AC system bus (CPF), constant DC voltage (CV), constant ignition angle (CIA), and constant extinction angle (CEA).

Most applications require that an HVDC converter be capable of both rectification and inversion. The control that makes this possible is shown in Fig. 6. Note that CIA and CEA are actually limits on CC control. Thus, these two control methods actually occur when the control demand forces the firing angle beyond its specified limits.

CC control can be simulated in a similar fashion as the tap changing under load control of reactive power flow. CC control is the capability of an HVDC converter to control the DC current flow through itself, another converter, or an HVDC line. The control equation would be of the form:

$$\Delta I_{pk} = \frac{\partial I_{pk}}{\partial \delta_p} \Delta \delta_p + V_p \frac{\partial I_{pk}}{\partial V_p} \frac{\Delta V_p}{V_p} + V_k \frac{\partial I_{pk}}{\partial V_k} \frac{\Delta V_k}{V_k} + \alpha_{pk} \frac{\partial I_{pk}}{\partial \alpha_{pk}} \frac{\Delta \alpha_{pk}}{\alpha_{pk}} \quad (26)$$

where α is the firing angle, p is the AC bus, and k is the DC bus of an HVDC converter controlling its own current. The firing angle is the start of conduction. The commutation angle is the completion of firing. Firing is the term used for conduction. If the control were implemented on a DC transmission line, the first term would not be present.

An HVDC converter controlling its own real power flow or that in another DC line is simulated by the following equation when bus p is the AC bus and k is the DC bus of the HVDC converter:

$$\Delta P_{pk} = \frac{\partial P_{pk}}{\partial \delta_p} \Delta \delta_p + V_p \frac{\partial P_{pk}}{\partial V_p} \frac{\Delta V_p}{V_p} + V_k \frac{\partial P_{pk}}{\partial V_k} \frac{\Delta V_k}{V_k} + \alpha_{pk} \frac{\partial P_{pk}}{\partial \alpha_{pk}} \frac{\Delta \alpha_{pk}}{\alpha_{pk}} \quad (27)$$

Note that if the HVDC converter were to be controlling a DC transmission line from bus p to bus k, the first term would not be present.

CPF control where a converter is controlling the AC system bus to which it is connected would be similar to the above control modes. If p is the AC bus and k the DC bus, because the power factor is related to the firing angle and the commutation angle (γ), then the control equation would be

$$\Delta PF_p = \alpha_{pk} \frac{\partial PF_p}{\partial \alpha_{pk}} \frac{\Delta \alpha_{pk}}{\alpha_{pk}} + \gamma_{pk} \frac{\partial PF_p}{\partial \gamma_{pk}} \frac{\Delta \gamma_{pk}}{\gamma_{pk}} \quad (28)$$

Note that the commutation angle has not been used previously as an independent variable, which will be discussed later. If the commutation angle or the firing angle were constant, then the respective term would not be present.

It is worthwhile to note that, for small power factor angles and commutation angles, equation 46may be simplified by using only the cosine of the firing angle. As both are generally small, equation 46arises because the fundamental of the square wave-like current waveform is approximately in phase with the current waveform. As the current waveform is displaced from the voltage waveform by approximately angle a, this angle becomes the power factor angle.

CV control of a DC bus can be simulated by a control equation that is a variation of the control equation of a TCUL transformer controlling the voltage magnitude of an AC bus. The partial derivative with respect to the DC bus voltage would be replaced by a partial derivative with respect to the firing angle. The bus equation of a DC bus k, connected to an AC bus p, and another DC bus q, would now be

$$\Delta P_k = \frac{\partial P_{pk}}{\partial \delta_p}\Delta\delta_p + V_p\frac{\partial P_{pk}}{\partial V_p}\frac{\Delta V_p}{V_p} + V_q\frac{\partial P_{kq}}{\partial V_q}\frac{\Delta V_q}{V_q} + \alpha_{pk}\frac{\partial P_{pk}}{\partial \alpha_{pk}}\frac{\Delta\alpha_{pk}}{\alpha_{pk}} \tag{29}$$

Note that the DC bus to be controlled does not have to be the DC bus to which the converter is connected.

The above equations had only the firing angle as an independent variable. The commutation angle can also be an independent variable if another equation can be added to the augmented Jacobian matrix. One method would be to find a unique relationship between the two angles. Another method would be to always constrain the current through a converter. If the current through a converter were constrained when real power flow control is in effect, then the two control equations would be

$$\Delta I_{pk} = \alpha_{pk}\frac{\partial I_{pk}}{\partial \alpha_{pk}}\frac{\Delta\alpha_{pk}}{\alpha_{pk}} + \gamma_{pk}\frac{\partial I_{pk}}{\partial \gamma_{pk}}\frac{\Delta\gamma_{pk}}{\gamma_{pk}} + \text{additional partial derivatives}$$

$$\Delta P_{pk} = \alpha_{pk}\frac{\partial P_{pk}}{\partial \alpha_{pk}}\frac{\Delta\alpha_{pk}}{\alpha_{pk}} + \gamma_{pk}\frac{\partial P_{pk}}{\partial \gamma_{pk}}\frac{\Delta\gamma_{pk}}{\gamma_{pk}} + \text{additional partial derivatives} \tag{30}$$

Note that only the partial derivatives that relate the two equations are shown here and not the partial derivatives that relate these control equations to the bus equations. The latter have been given previously. It is only a direct copy of the above scheme to include CC control with CPF or CV control.

The relationship between the firing and commutation angles for the controlled cases is a more difficult matter and is omitted here. The recent text by Arrillaga is the classic reference for HVDC modeling [x].

Modeling of Transmission Lines and Transformers

Transmission Line Flow Equations. Transmission lines are modeled as shown in Fig. 7. The flow as measured at each end of each transmission line is given in the following equations.

Given the voltage at each end of the transmission line:

$$\text{Voltage at bus } i : V_i = |V_i|\langle\delta_i$$

$$\text{Voltage at bus } j : V_j = |V_j|\langle\delta_j$$

Given the series and the shunt impedance of the line:

$$\begin{aligned}\text{Series impedance}: &\quad y_{ij} = |y_{ij}|\langle\gamma_{ij}\\ \text{Shunt impedance}: &\quad y_{ij} = |y_{ij}|\langle 90^\circ\end{aligned}$$

Then the current from bus i to bus j measured at bus i is

$$\begin{aligned} I_{ij} &= V_i y_{ij} + (V_i - V_j)y_{ij}\\ &= V_i(y_{ii} + y_{ij}) - V_j y_{ij}\end{aligned} \tag{31}$$

The power flowing from bus i to bus j measured at bus i is

$$S_{ij} = V_i I_{ij}^* \tag{32}$$

Substituting the current relationship:

$$S_{ij} = |V_i|^2 y_{ii}^* + |V_i|^2 y_{ij}^* - V_i V_j^* y_{ij}^* \tag{33}$$

It simplifies to

$$P_{ij} = |V_i|^2|y_{ii}|cos(\gamma_{ij}) - |V_i||V_j||y_{ii}|cos(\delta_i - \delta_j - \gamma_{ij}) \tag{34}$$

$$Q_{ij} = -|V_i|^2|y_{ij}| - |V_i|^2|y_{ii}|sin(\gamma_{ij}) - |V_i||V_j||y_{ii}|sin(\delta_i - \delta_j - \gamma_{ij}) \tag{35}$$

These equations are used as the starting point for all partial derivatives.

Transformer Flow Equations. Transformers are modeled as shown in Fig. 8. The flow as measured at each end of the transformer is given in the following equations.

Given the voltage at each end of the transformer:

$$V_k = V_m(1\langle\theta)$$

$$V_m = \alpha V_j \tag{36}$$

Given the series impedance and tap of the transformer:

$$\begin{aligned}\text{Series impedance}: y_{ij} &= |y_{ij}|\langle\gamma_{ij}\\ \text{Tap ratio}: \alpha_{ij} &= |\alpha_{ij}|\langle 0^\circ\end{aligned}$$

Then the current from bus i to bus j measured at bus i is

$$\begin{aligned} I_{ij} &= (V_i - V_k)Y_{ij}\\ I_{ij} &= V_i Y_{ij} - V_k Y_{ij}\end{aligned}$$

$$\begin{aligned} I_{ij} &= V_i Y_{ij} - V_m(1\langle\theta)Y_{ij}\\ I_{ij} &= V_i Y_{ij} - \alpha_{ij} V_j(1\langle\theta)Y_{ij}\end{aligned} \tag{37}$$

Note that α is a real number in this model. It may also include an angle for a phase-shifting transformer (QPS).

Correspondingly for the other bus:

$$\begin{aligned} P_{ji} &= -\alpha|V_i||V_j||Y_{ij}|\cos(\theta_i - \theta_j - \theta + \theta_{ij}) + \alpha^2|V_j|^2|Y_{ij}|\cos\theta_{ij}\\ Q_{ji} &= \alpha|V_i||V_j||Y_{ij}|\sin(\theta_i - \theta_j - \theta + \theta_{ij}) - \alpha^2|V_j|^2|Y_{ij}|\sin\theta_{ij}\end{aligned} \tag{38}$$

Other models are also used depending on how the transformer was built, what variable tap positions are available, and how the transformer is connected into the transmission grid. Transformers are used to control voltages, real power flows, and (rarely) reactive flows.

Note that the flow equations are the normal starting point to find the partial derivatives necessary for the Jacobian matrix within industrial programs.

Modeling of HVDC Converters and FACT Devices

The limitations of current technology require that a converter draw substantial amounts of reactive power from the AC system to which it is connected. Significant amounts of reactive power are supplied by capacitors. Additionally, passive and active filters are added to remove unwanted harmonic interaction. Such device modeling is found in the literature [x].

Definition of Angular Relationships. The primary concept is to find a relationship between the real and the reactive flows with respect to the system voltage magnitudes and angles and any controlling parameters, such as firing angle and commutation angle. It is necessary to be able to find the first partial derivatives of these flows with respect to the voltages and the control variables. The same is true for many FACT device because most such devices are back-to-back A/D/AC converters.

The complete, steady-state internal operation of a converter can largely be described by two quantities: the firing angle α and the commutation angle γ. Figure 9 shows the relationships between the commonly defined angles for the six-pole converter equivalent circuit shown. This description uses the firing angle α to describe the converter mode of operation: rectification or inversion.

Power Equations for a Six-Pole HVDC Converter. Representative Jacobian entries for an HVDC converter are presented. The analysis is significantly simplified if the following assumptions are used. The firing voltage and the arc-drop voltage are negligible, (i.e., ideal diodes). The operation of an adjacent bridge has no effect on any other bridge. This comment is applicable when several bridges are connected in series to make up the total installation. The direct current is constant and ripple-free. The power system is a balanced three-phase sinusoidal voltage of constant magnitude and frequency (infinite bus). The source impedance may be lumped with the converter transformer. The magnetizing and eddy current components of the transformer are negligible. The converter has minimal active power loss (the commutating resistance Rk is negligible).

The power for the AC side of the converter is written as

$$\begin{aligned} S_{3\Phi} &= \sqrt{3} V_{LL} I^* = P_{3\Phi} + jQ_{3\Phi} \\ P_{3\Phi} &= |V_{LL}| V_{DC} X'_k \phi_1 \\ Q_{3\Phi} &= \frac{1}{2} |V_{LL}| V_{DC} X'_k \phi_2 \end{aligned} \tag{39}$$

$$\begin{aligned} |V_{LL}| &= \lfloor V_{LL} \sin(\delta)^2 + V_{LL} \cos(\delta)^2 \rfloor \, 1/2 \\ \phi_1 &= \cos(\alpha) - \cos(\alpha + \gamma) \end{aligned}$$

$$\begin{aligned} \phi_2 &= \frac{\gamma - \sin(\gamma) \cos 2(\alpha + \frac{\gamma}{2})}{\cos(\frac{\gamma}{2}) \cos(\alpha + \frac{\gamma}{2})} \\ X'_k &= (\sqrt{2} X_k)^{-1} \end{aligned} \tag{40}$$

Note that $P_{3\phi}$ and $Q_{3\phi}$ do not depend on the bus voltage angle with respect to the swing bus. At the DC side,

$$P_{DC} = V_{DC} I_{DC} = -P_{3\phi} \tag{41}$$

Thus, the following partial derivatives are easily derived. The terms for the AC bus are:

$$\begin{aligned} |V_{LL}| \frac{\partial P_{3\phi}}{\partial |V_{LL}|} &= P_{3\phi}, \quad \frac{\partial P_{3\phi}}{\partial \delta} = 0.0 \\ |V_{LL}| \frac{\partial Q_{3\phi}}{\partial |V_{LL}|} &= Q_{3\phi}, \quad \frac{\partial Q_{3\phi}}{\partial \delta} = 0.0 \\ V_{dc} \frac{\partial P_{3\phi}}{\partial V_{DC}} &= P_{3\phi}, \qquad V_{DC} \frac{\partial Q_{3\phi}}{\partial \delta} = Q_{3\phi} \end{aligned} \tag{42}$$

The terms for the DC bus are

$$\begin{aligned} V_{DC} \frac{\partial P_{DC}}{\partial V_{DC}} &= P_{DC} \\ |V_{LL}| \frac{\partial P_{DC}}{\partial |V_{LL}|} &= P_{DC}, \quad \frac{\partial P_{DC}}{\partial \delta} = 0.0 \end{aligned} \tag{43}$$

These derivatives are needed for the Jacobian matrix.

Brief Comments on Jacobian Matrix Processing

The full details of the manipulation of the Jacobian will not be given here because these details are well documented in the literature (8–11). A brief procedure is shown in Table 2.

The elementary form of the correction to the bus voltage vector is simply the factorization of the Jacobian matrix, augmented with the real and reactive residuals. After the factorization, the updates to the voltage magnitudes and angles are found in the column where the residuals were located.

The inclusion of DC links causes the voltage magnitude update vector to increase in dimension without increasing the dimensionality of the vector $\Delta\delta$. Similarly, the ΔP vector increases in dimension, but the ΔQ vector does not. Hence, the Jacobian remains square, but the dimensions of the submatrices differ.

The digital computer solution is divided into the following functions:

1. Form the Jacobian matrix.
2. Augment the Jacobian with the column vector.
3. Solve the augmented Jacobian matrix for the correction vector.
4. Update the solution vector.

Three functions are typically used: SETUP_J, SOLVE_J, and NEWVAR.

Setup J.
This function has two major functions:

1. Build the augmented Jacobian matrix (AJM).
2. Check each equation for solution within a specified tolerance.

SETUP_J builds the augmented Jacobian matrix bus-by-bus. All partial derivatives for a bus are calculated simultaneously with the flow calculations to determine the mismatch. The mismatch is actually the error for the equations. A chain-linked data structure is used to conserve space used.

Solve J.
This function performs Gaussian elimination and back-substitution on the AJM using sparcity programming and chain-linked data techniques. An unusual feature is the limit status, which contains a code that is used to determine whether one, two, or no equations are associated with each bus. The corrections are left in memory for the variable updating routine. Note that, as control variables hit limits, the control may be relaxed and afterward reinstated.

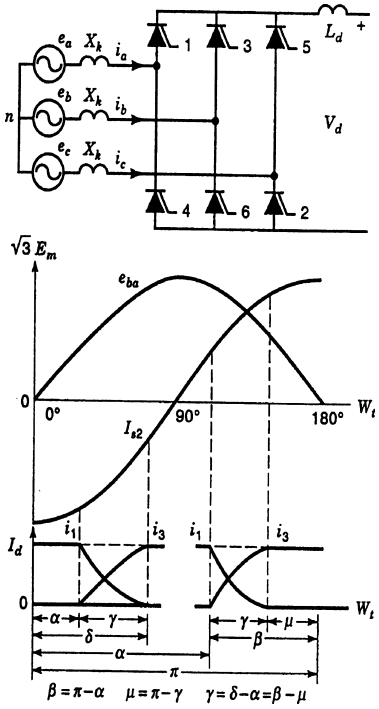

Figure 9. (a) HVDC converter basic circuit. (b) HVDC converter angle relationships.

Newvar.

This function updates the independent variables (voltage magnitude and angle) by applying the corrections calculated by the solution subroutine. The corrected variables are left in core for the building subroutine.

Decoupled Power Flow (Stott)

The decoupled power flow is the most popular technique and is from the research of Brian Stott [x]. If one is aware that the node/bus volt magnitudes are approximately unity, that the bus angles are nearly the same, and that the susceptance is much larger than the per-unitized reacitve flow, then the following simplifications result:

$$B\prime = \frac{\partial P_i}{\partial \delta_i} \tag{44}$$

$$B\prime\prime = \frac{\partial Q_i}{\partial V_i} \tag{45}$$

The net result is that the Jacobian is now decoupled between the real equations and the reactive equations:

$$\begin{aligned} \Delta P &= B\prime \Delta\delta \\ \Delta Q &= B\prime\prime \Delta V \end{aligned} \tag{46}$$

Additionally, the Jacobian elements do not have to be recalculated each iteration. The computational savings is enormous for practical size systems.

DC Power Flow

The DC power flow is a suitable planning technique. If one is aware that the node/bus volt magnitudes may be treated as approximately unity, then the reactive equations may be ignored or solved later when the reactive demand is known:

$$B\prime = \frac{\partial P_i}{\partial \delta_i} \tag{47}$$

The net result is that the Jacobian is now a single relationship between the real power and the voltage angle:

$$\Delta P = B\prime \Delta\delta \tag{48}$$

Additionally, the Jacobian elements do not have to be recalculated each iteration. The computational savings is enormous for practical size systems.

Element Compensation Theorem

One interesting breakthrough was based on the need to not alter the Jacobian matrix or to resolve for the table of factors for the Jacobian matrix as the system parameters or configuration changed as devices were removed, added, or the control parameters altered. The basis of the technique is most easily shown by the following figures as shown in Wood and Wollenberg and Carpentier [xx, yy]. Figure 10a shows the original configuration with the solved real and reactive power flows shown as $P(i,j)$ and $Q(i,j)$.

Figure 10b shows the new configuration with the circuit breakers (switches) open at both ends of the line as it is removed from service. Now the flows from bus m to bus n should be zero.

Figure 10c shows the equivalent network with the addition of artificial injections to remove the flows from the solution. The theory is that the line flows $[P(m,n), Q(m,n)]$ are matched by the equivalent injection at bus m and the line flows $[P(n,m), Q(n,m)]$ are matched by the equivalent injection at bus n. Thus, the equivalent injections have effectively removed the line flows from the solution. The

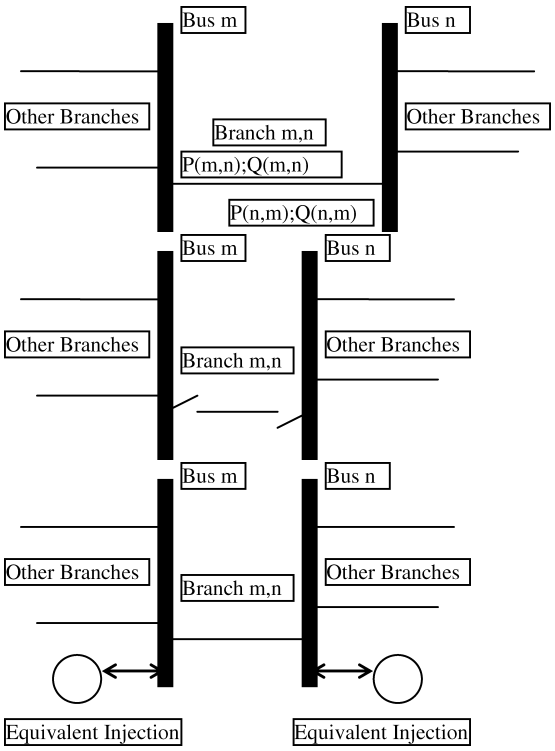

Figure 10. (a) One line diagram for branch compensation algorithm–original configuration. (b) One line diagram for branch compensation algorithm–open line. (c) One line diagram for branch compensation algorithm–equivalent model.

same idea may be applied to any series device if the parameters change is associated with that device, such as TCUL transformers. This saves the computational effort to reform the Jacobian matrix and to refactor that matrix.

The key assumption to applying this technique is that both buses are still part of the same power system. Essentially, one has to check that the system has not been split into two power systems by the removal of a critical component.

EXAMPLE SYSTEM

Introduction

In this section, a small power system is used to exemplify the effect of the addition of alternative link devices. The six-bus AC Ward and Hale system [x5] is augmented with a single monopolar HVDC line. All values are given in per-unit.

Ward and Hale System

The single line diagram for the Ward and Hale six-bus system is shown in Fig. 11. The reference bus is bus number one with the specified values given in Table 3. Note that all values are given as per-unit quantities. The line data and the line power flows are contained in Tables 4 and 5, respectively. The TCUL transformers were represented by equivalent pi parameters.

The structure of the corresponding Jacobian matrix is shown in Fig. 12. Note that the first row and column are not present because Bus 1 is the slack bus. As discussed below, the Jacobian matrix is the first partial derivative of the line flows with respect to the voltage magnitude or angle. The following notation is used. ΔP is the real mismatch. ΔQ is the reactive power mismatch, Δd is the angular update to voltage. ΔV is the magnitude update to voltage. H $(\partial P/\partial d)$ is the partial derivative of the real power to the angular update. N $(\partial P/\partial V)$ is the partial derivative of the real power to the voltage magnitude update. M $(\partial Q/\partial d)$ is the partial derivative of the reactive power to the voltage update. L $(\partial Q/\partial V)$ is the partial derivative of the reactive power to the voltage magnitude update. Note that many zero entries exist. Large systems of 2500 to 5000 buses have a large percentage of nonzero entries. It is typical for the Jacobian matrix to have 80% to 90% zero entries. Such a fortunate structure has been exploited through sparcity programming to significantly reduce the computer resources needed for solution.

The addition of a DC monopolar line from Bus 2 to Bus 6 would appear as in Fig. 14. Note that the submatrix J' is the original matrix shown in Fig. 11. The system of partial differential equations (SPDE) of Fig. 12 would be enlarged with the addition of the partial derivatives shown in Fig. 14. The line data for the DC link is given in Table 6. It is also necessary to add reactive capability at Bus 2 and at Bus 5. These increases are shown in Table 7. The resulting flows are shown in Tables 8 and 9.

The previous system is only an academic utilization of the model developed herein. Actual system studies would include a transformer between the system AC bus and the converter AC bus. Then the DC system would be more of the form shown in Fig. 15. Filters and reactive power supplies

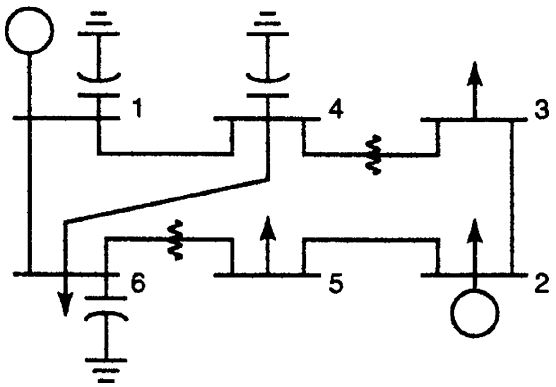

Figure 11. Ward–Hale six-bus power system.

ΔP_2		H_{22}	N_{22}	H_{23}	N_{23}			H_{25}	N_{25}				$\Delta\delta_2$
ΔQ_2		M_{23}	L_{23}	M_{23}	L_{23}			M_{25}	L_{25}				$\Delta V_2/V_2$
ΔP_3		H_{32}	N_{32}	H_{33}	N_{33}	H_{35}	N_{35}						$\Delta\delta_3$
ΔQ_3		M_{32}	L_{32}	M_{33}	L_{33}	M_{35}	L_{35}						$\Delta V_3/V_3$
ΔP_4				H_{43}	N_{43}	H_{44}	N_{44}			H_{46}	N_{46}		$\Delta\delta_4$
ΔQ_4	=			M_{43}	L_{43}	M_{44}	L_{44}			M_{46}	L_{46}	*	$\Delta V_4/V_4$
ΔP_5		H_{52}	N_{52}					H_{55}	N_{55}	H_{56}	N_{56}		$\Delta\delta_5$
ΔQ_5		M_{52}	L_{52}					M_{55}	L_{55}	M_{56}	L_{56}		$\Delta V_5/V_5$
ΔP_6						H_{64}	N_{64}	H_{56}	N_{56}	H_{66}	N_{66}		$\Delta\delta_6$
ΔQ_6						M_{64}	L_{64}	M_{56}	L_{56}	M_{66}	L_{66}		$\Delta V_6/V_6$

Figure 12. Jacobian matrix.

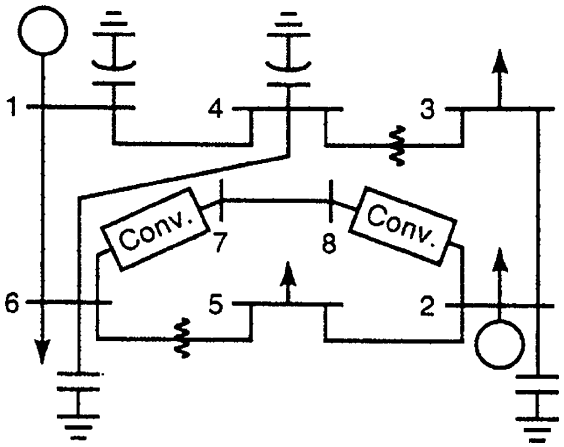

Figure 13. Ward–Hale power system with HVDC link.

can be added as injected powers, currents, or impedance loads at the bus (AC or DC) to which it is connected.

EXTENSIONS

Many extensions to the above basic power flow description are used in industrial solutions on a daily basis.

Visualizations

Visualization of the power system data refers to presentation of the data to help users create a mental picture of the system. Such presentations assist users to analyze the results and extract desired information much more efficiently. Today, engineering models of electrical network consist of thousands of buses and line. This high dimensionality of the power network makes the task of visualization even mere important and challenging.

The most common form of an electrical network representation has been one-line diagrams. The man–machine interface (MMI) of a traditional energy management system (EMS) depicts the network connections using one-line diagrams. The MMI pictures have two kinds of components: static and dynamic. The static components consist

ΔP_2		H_{22}	N_{22}	H_{23}	N_{23}			H_{25}	N_{25}						$\Delta\delta_2$
ΔQ_2		M_{23}	L_{23}	M_{23}	L_{23}			M_{25}	L_{25}						$\Delta V_2/V_2$
ΔP_3		H_{32}	N_{32}	H_{33}	N_{33}	H_{35}	N_{35}								$\Delta\delta_3$
ΔQ_3		M_{32}	L_{32}	M_{33}	L_{33}	M_{35}	L_{35}								$\Delta V_3/V_3$
ΔP_4				H_{43}	N_{43}	H_{44}	N_{44}			H_{46}	N_{46}				$\Delta\delta_4$
ΔQ_4				M_{43}	L_{43}	M_{44}	L_{44}			M_{46}	L_{46}				$\Delta V_4/V_4$
ΔP_5		H_{52}	N_{52}					H_{55}	N_{55}	H_{56}	N_{56}				$\Delta\delta_5$
ΔQ_5	=	M_{52}	L_{52}					M_{55}	L_{55}	M_{56}	L_{56}			*	$\Delta V_5/V_5$
ΔP_6						H_{64}	N_{64}	H_{56}	N_{56}	H_{66}	N_{66}				$\Delta\delta_6$
ΔQ_6						M_{64}	L_{64}	M_{56}	L_{56}	M_{66}	L_{66}				$\Delta V_6/V_6$
ΔP_7										H_{67}	N_{67}	H_{77}	H_{78}		ΔV_7
ΔP_8		H_{28}	N_{28}									H_{87}	H_{88}		ΔV_8

Figure 14. Jacobian matrix with HVDC link.

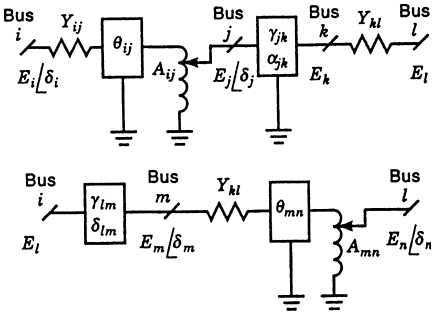

Figure 15. Converter DC system with phase shifters.

of texts and symbols. A text describes the title of a network parameter, such as bus voltage magnitude and real power loss. A symbol represents a network component, such as generator and breaker. The dynamic components consist of values of network solution parameters to describe system conditions and status of breakers and switches. The numerical values of network solution parameters are written next to the associated network components shown in the one-line diagram. The breaker status is usually color-coded and is dynamically updated to describe the network topology. A common additional feature available in an MMI is that generation of an alarm when a computed or telemetered value exceeds its limit. This alarm is intended to catch the operator's immediate attention.

Additional visualizations include spider diagrams, transmission path coloring by loading level, reactive power islands by color, and others.

Harmonic Analysis

Extensions to harmonic analysis are required because of the inclusion of the power electronic devices. The basic works by Arrillaga, MacGrady, and others have extended the power flow to frequencies other than 50 or 60 Hz to include the multiple harmonics generated by power electronic devices.

A conventional power flow is a method of determining the line power flows and the system bus voltages in terms of a given system generation and load configuration. The conventional power flow is used in power system planning and design, reliability considerations, system generation and load evaluation, and other power system applications. Harmonic power flows that have been applied to terrestrial systems are being used for system design and reliability considerations. The terrestrial harmonic power flow then examines what effects these nonlinear loads have on the power system in terms of producing high-voltage and current levels, resonant conditions, communication interferences, and protection relay interferences.

Harmonic power flows in general require the same system data that are used by a conventional power flow, which includes line and transformer parameters, system generation and load data, and how the system is connected. In addition, harmonic power flows also require data on the nonlinear loads, as in equivalent impedance data, power requirements, and type of nonlinearity that the load generates. However, harmonic power flows are much more complex than conventional power flows because they do allow the inclusion of these nonlinear loads and devices. This, in essence, makes a harmonic power flow a type of generalized power flow that can, in addition to calculating the system line flows and bus voltages, analyze the effect nonlinear loads can have on a power system. This process makes the harmonic power flow a valuable tool in power system analysis and design.

Security Boundary Characterization

Transmission networks are operating closer to their limitations as the power industry is restructuring around the

world. Security assessment through boundary visualization provides the knowledge of system security levels in terms of easily visualized operating parameters. New research is ongoing to find a methodology for on-line security boundary visualization using neural networks. Such methodology models the traditional security assessment procedures that result in a nomogram for characterizing the security boundaries.

The power industry is restructuring from regulation to deregulation. One new challenge is how to appropriately evaluate the security levels of the current operating conditions when the system is being operated closer to its limitations because of heavy use of the transmission network. In this new environment, security assessment for the transmission network must be accurate and easily accessed online by system operators.

Security assessment can be divided into two levels: classification and boundary determination. Classification involves determining whether the system is secure or insecure. Classification does not indicate distance from the current condition to the insecure conditions.

Boundary determination, on the other hand, involves measuring this distance. A boundary is represented by constraints imposed on parameters defining precontingency conditions. These precontingency parameters are called critical parameters. Once the boundary is identified, security assessment for any operating point can be given as the "distance" (in terms of critical parameters) between the current operating point and the boundary. Assessment in terms of precontingency operating parameters instead of the postcontingency performance measure is more meaningful (1, 2). Many North American utilities use the traditional boundary characterization approach to generate a two-dimensional graph called a nomogram (3–5). A nomogram has two axes corresponding to two critical parameters.

Voltage Stability in Power Systems—An Overview

There has been an increasing interest and investigation into voltage instability and collapse. As this interest has spawned research, the literature has also grown. The first paper related to voltage instability appeared in 1968 (18). Venikov (6) proposed the first criteria for detecting the point of voltage collapse. Voltage instability has been a known problem for a long time. However, active research involving voltage stability did not start in earnest until the 1980s.

The references are divided by information content into groups (5). The most pertinent references are listed here; a thorough report is in the bibliography by Ajjarapu et al. (5). The first group includes books (1–4) related to voltage stability. The second group lists in alphabetic order the papers (19–42) directly related to voltage stability.

The imbalance between load growth and generation and transmission expansion grew during the 1970s and 1980s. The problem of voltage stability and voltage collapse has been a major area of attention in North America. Voltage stability is the ability of a power system to maintain steady acceptable voltages at all buses in the system under normal operation conditions and after being subjected to a disturbance. A system enters a state of voltage instability when a disturbance, increase in load demand, or change in system condition caused a progressive and uncontrollable drop in voltage. The crux of the problem is the voltage drop that occurs when excessive power flows through the inductive reactances of the transmission lines and transformers because of increased loading.

The model for analyzing voltage stability should include all components that effect voltage. Some believe the structure-preserving model is the most appropriate for this analysis, even-though initial research concentrated only on power flow analysis. Analytically, Venikov proposed one of the first criteria for detecting the point of voltage collapse as the point where the determinant of the Jacobian of power flow equations becomes singular. Continuation-based power flow analysis is a promising approach for robust static analysis.

Various indices and approaches have been proposed. It is not just sufficient to understand and analyze the voltage collapse phenomena; it is essential that effective, economically justified solutions to the voltage problems be developed. The challenge for future research is to come up with preventive and corrective control strategies for on-line prediction and control to mitigate voltage collapse. Another challenge is to integrate some of these strategies for on-line ATC calculations as limited by voltage stability.

BIBLIOGRAPHY

1. Ekstrom, A.; Danfors, P. Future HVDC Convertor Station Design Based on Experience with the World's First Thyristor Installation Proc.; *American Power Conference*; 1973, pp 1153–1159.
2. The Representation of an HVDC Link in a Network Analyser.
3. Uhlmann, E. Paper 404, *Conference Internationale des Grands Reseaux Electriques a Haute Tension*; 1960.
4. Dougherty, J. J.; Caleca, V. The EHI A/DC Transmission Model. *IEEE Power Apparat. Syst.*, 1968, **87**, p 504.
5. Lipo, T. A. Analog Computer Simulation of a Three-Phase Full-Wave Controlled Rectifier Bridge. *Proc. IEEE* 1969, **57**.
6. Clifford, J. F.; Schmidt, Jr. A. H., Digital Representation of a DC Transmission System and its Controls. *IEEE Power Apparat. Syst.*, 1970, **PAS-70**, pp 97–105.
7. Stagg, G. W.; El-Abiad, A. H. *Computer Methods in Power System Analysis*; McGraw-Hill: New York, 1968, Chapter 8.
8. Vithayathil, J. J. Digital Simulation of DC Systems for Load Flow and Transient Stability Studies.February 1970, Draft of a paper, along with program documentation provided by W. F. Tinney of Bonneville Power Administration.
9. Tinney, W. P.; Walker, J. W. Direct Solutions of Sparse Network Equations by Optimally Ordered Triangular Factorization. *Proc. IEEE*, 1967, **55**, pp 1801–1809.
10. Tinney, W. F.; Hart, C. E. Power Flow Solution by Newton's Method. *IEEE Power Apparat. Syst.*, 1967, **PAS-86**, pp 1449–1460.
11. Ogbuobiri, E. C. Dynamic Storage and Retrieval in Sparcity Programming. *IEEE Power Apparat. Syst.*, 1970, **PAS 89**, pp 150–155.
12. VanNess, J. E. Iteration Methods for Digital Load Flow Studies. *AIEE Trans.*, 1959, **78**, pp 583–588.

13. Britton, J. P. Improved Area Interchange Control for Newton's Method Load Flows. *IEEE Power Apparat. Syst.*, 1969, **PAS-88**, pp 1577–1581.
14. Britton, J. P. Improved Load Flow Performance Through a More General Equation Form. *IEEE Power Apparat. Syst.*, 1971, **PAS-71**, pp 109–116.
15. Peterson, N. M.; Meyer, W. S. Automatic Adjustment of Transformer and Phase Shifter Taps in the Newton Power Flow. *IEEE Power Apparat. Syst.*, 1971, **PAS-71**, pp 103–108.
16. Kimbark, E. W. *DC Transmission*, Vol.**I**; Wiley-Interscience: New York, 1971.
17. Neiman; Glinternik; Emelyanov; Novitskii. DC Transmission in Power Systems. Translated from Russian by Israel Program for Scientific Translations, Jerusalem, 1967, available from Clearinghouse for Federal Scientific and Technical Information, Springfield, VA.
18. Hingorani, N. G. Operating Experience of the Pacific Northwest-Southwest HVDC Intertie; *Proc. American Power Conference*; 1973, pp 1160–1169.
19. VanNess, J. E.; Griffin, J. H. Elimination Methods for Load Flow Studies. *Trans. AIEE*, 1961, **80**, p. 299.
20. Gross, C. E. *Power System Analysis*; Wiley: New York, 1985.
21. Heydt, G. T. *Computer Analysis Methods for Power Systems*; Stars in a Circle Publications: Scottsdale, AZ, 1996.
22. Wood, A. J.; Wollenberg, B. J. *Power Generation Operation & Control*; Wiley: New York, 1997.
23. Glover, J. D.; Sarma, M. Power System Analysis and Design; PWS Publishers: Boston, MA, 1987.
24. Harmonic Power Flow Studies. EPRI Report. EL-3300 Project 1764-7, 1983.
25. Grady, W. M. Harmonic Power Flow Studies. Doctoral Dissertation, Purdue University, August 1983.
26. Wood, J.; Wollenberg, B. F. *Power Generation, Operation, and Control*; Wiley: New York, 1984.
27. Arrillaga, J.; Bradley, D. A.; Bodger, P. S. *Power System Harmonics*; Wiley: New York, 1985.
28. Mahmoud; Shultz, R. D. A Method for Analyzing Harmonic Distribution in AC Power Systems. *IEEE Trans. Power Apparat. and Syst.*, 1982, **PAS-101**.
29. Blackwell, W. A.; Grigsby, L. L. *Introductory Network Theory*; PWS Engineering, 1985.
30. Glasscock, T. C. *A Generalized Admittance Matrix Approach to the Steady State Analysis of Spacecraft Power Systems*. Masters Thesis, Auburn University, 1989.
31. Williamson, F.; Sheble, G. B. Single Phase Harmonic Analysis of Spacecraft Power Systems Using a Personal Computer; *Proc. 21/2st Southeastern Symposium on System Theory*; Tallahassee, FL, March 1989.
32. Shepherd, W.; Zand, P. *Energy Flow and Power Factor in Nonsinusoidal Circuits*; Cambridge University Press: Cambridge, UK, 1979.
33. Rashid, M. H. *Power Electronics*; Prentice Hall: Englewood Cliffs, NJ, 1988.
34. Arrillaga, J.; Watson, N. R. *Computer Modeling of Electrical Power Systems*; Wiley: New York, 2001.
35. Arrillaga, J.; Watson, N. R. *Power System Harmonics*; Wiley: New York, 2003.
36. Arrillaga, J.; Smith, B. C.; Watson, N. R.; Wood, A. R. *Power System Harmonic Analysis*; Wiley: New York, 1997.
37. Glover, J. D.; Sarma, M. S. *Power System Analysis and Design*; Thomson-Engineering: New York, 2001.
38. Saadat, H. *Power Systems Analysis*; McGraw-Hill: New York, 2002.
39. Bergen, A. R.; Vittal, V. *Power Systems Analysis*; Prentice Hall: Englewood Cliffs, NJ, 1999.
40. Gross, C. A. *Power System Analysis*; Wiley: New York, 1986.
41. Mohan, N. First Course on Power Systems. Minnesota Power Electronics Research & *Education* (MNPERE), 2006.
42. Carpentier, J. W. Differential Injections Model, a General Method for Secure and Optimal Load Flows 1975 PICA Conference Proc.; pp 255–262.

Reading List

Adamson; Hingorani, N. *HVDC Transmission*; Garraway, 1960.

Ward, J. B.; Hale, H. W. Digital Computer Solution of Power-Flow Problems. *AIEE Trans.*, 1956, **75**, pp 398–404.

Ogbuobiri, E. C.; Tinney, W. P.; Walker, J. W. Sparcity-Directed Decomposition for Gaussian Elimination on Matrices. *IEEE Power Apparat. Syst.*, 1970, **PAS 89**, pp 141–150.

Brown, H. E. *Solution of Large Networks by Matrix Methods*; Wiley: New York, 1975.

Brown, R. J.; Tinney, W. F. Digital Solution for Large Power Networks. *Trans. AIEE*, 1957, **76**, pp 347–355.

Elgerd, O. I. *Electric Energy Systems Theory: An Introduction*; McGraw-Hill: New York, 1971.

Grainger, J.; Stevenson, Jr. William, D. *Power Systems Analysis*; McGraw-Hill: New York, 1994.

Sato, N.; Tinney, W. F. Technique for Exploiting the Scarcity of the Network Admittance Matrix. *Trans. IEEE PAS*, 1963, **82**, p. 944.

GERALD B. SHEBLÉ
Portland State University
Portland, OR